Optimal Design of Power-train Mounting Systems using Generalized Force Transmissibility

Yanan Wang*, Xin He, Yue Liu, Kuigang Yu

School of Mechanical Engineering, Key Laboratory of High-efficiency and Clean Mechanical Manufacture, Ministry of Education, Shandong University, Jinan, China

Abstract — we examine the optimization of Power-train Mounting Systems (PMSs) and study Generalized Force Transmissibility (GFT) considering the excitation and vibration properties of power-trains. The Sum of Generalized Force Transmissibility Integrals (SGFTI) of a PMS is defined for vibration isolation index of the system. Using SGFTI as the objective and adding necessary constraints, we optimize the design variables of position, orientation and stiffness of the mounts with Generalized Reduced Gradient (GRG) algorithm. To investigate the characteristics of this method, a typical PMS is optimized with full constraints and with less constraints successively. The results show the relationship and different properties of this method and the widely used Torque Roll Axis (TRA) method. Mounts and their brackets are then modified and redesigned according to the optimization results, and the feasibility and effectiveness of this method are proved by tests. Compared to other optimal design methods of PMSs, the GFT method can improve the vibration isolation performance directly in the required frequency ranges when the design space is very limited, and no complicated input caculations or measurements are needed. It is a desirable optimal method to improve the design stage of PMSs.

Keywords - power-train, mounting system, optimal design, vibration isolation, Sum of Generalized Force Transmissibility Integrals.

I. INTRODUCTION

A PMS is typically composed of a power-train and a certain number of resilient mounts. For most vehicles, the power-train is one of the heaviest qualities and the main sources of vibration. The excitations and the vibrations of the power-train may cause serious vibrational and acoustic problems on the body system, so an elastic and restraining mounting system should be effectively set between the power-train and its foundation, sometimes even independent damping elements are needed.

The vibration responses of a PMS mainly depend on its excitations and characteristic parameters, such as the inertia, the elasticity and the damping, etc. The inertia of a power-train is determined by its structure and density, which are usually set already before the design stage of the mounting system. The damping is usually provided by the mounting system, but most rubber mounts can only provide very limited damping effects, which are also difficult to be considered as independent design variables. The major excitations generally include the torques around the driven shaft axis and the inertial forces along the direction of acceleration or gravity. For traditional-energy vehicles and some new-energy vehicles such as hybrids and alternative fuels, they mainly include overturning torques and reciprocating inertial forces generated from the internal combustion engines. For vehicles powered by electric motors, torque and force fluctuations generated from the motors and their inertia may take major part when they are started or on the road. But the exact values of these excitations are not easy to get by calculations [1] or even measurements [2, 3]. All of these negative factors make the optimization of a PMS into a difficult task. However, the mounting elasticity is determined by the stiffness, the positions and the orientations of the mounts, and these parameters normally can be obtained and modified easily in the design stage. Therefore, the optimization of a rubber mounting system is usually committed to lowering the vibration level by means of adjusting the stiffness, the position, and the orientation of each mount properly, meanwhile satisfying the load-bearing and durability requirements in the process [4].

For PMSs on vehicles, there has been no uniform evaluation index of their vibration isolation performance yet, so the optimal design objectives are also various. Researchers and engineers have proposed different principles and methods from different perspectives. Among them, one of the most widely used is the TRA method [3, 5] and the related Modal Kinetic Energy (MKE) method [6, 7], even in the mounting design of electric vehicles [8]. Jeong T. and Singh R. proposed the TRA method for the scheme design of PMSs [5]. The roll mode around the TRA is the main form of movement excited by the pulsating torques. This method aims at decoupling this mode from other physical modes, for the reason that a decoupled system produces fewer resonances over the operating range. However, this method does not pay special attention to the vertical and pitch modes of the power-train, which may be easily excited by inertial forces in vertical direction. For this reason, the MKE method pursues to decouple all the 6 modes of the rigid-body vibration of a PMS, as well as a reasonable distribution of the modal frequencies, but it is not easy to be achieved on real vehicles because of the very limited design space. Besides, for a PMS with multiple mounts, multiple degrees of freedom and multiple kinds of excitations, the evaluation indices of both methods—MKE distribution cannot clearly indicate its vibration isolation performance. Other optimizations often use certain kinds of

responses as indices, such as the force transmitted to the basis [1], the centroid displacement of the power-train [9], and the Frequency Response Function by tests [10], etc., but real responses often involve experimental tests or the calculations of excitations. Tests raise design costs, and the excitations are very difficult to be accurately calculated because of the complexity of the power-train, such as transmissions, fluid torque converters or torsional vibration dampers.

In view of the above aspects, this research proposes a series of GFT functions to clearly indicate the vibration isolation performance of a PMS. The definition of SGFTI and the related optimal design method pursuing its reduction are brought out, which can lower the system GFT level within very limited design space, and no experimental tests or excitation calculations are needed. The calculation and optimization procedures of this method are illustrated in details, and the features and effects, especially the relations with the TRA method, are discussed by the examples and their comparison, and then verified in tests.

II. OPTIMAL DESIGN METHOD REGARDING GENERALIZED FORCE TRANSMISSIBILITY

A. Generalized Force Transmissibility of a Mounting System

As mentioned above, the major types of excitations of a power-train include pulsating torques and inertial forces. The two types of excitations are applied on the power-train as torque and force fluctuations, causing vibrational rotations and translations about/of the mass center. Consequently dynamic forces are transmitted to the foundation through the mounts in the mounting system, which may bring about vibrational or acoustic problems of the vehicle, as shown in Fig. 1.

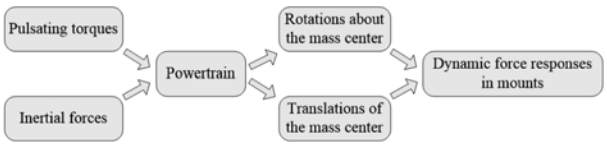

Figure 1. The vibration mechanism of a PMS

Besides the excitations, the dynamic force responses in the mounts also depend on the natural vibration characteristics of the PMS, and the affecting factors include the stiffness, the positions and the orientations of the mounts as well as the inertia parameters of the power-train, such as the mass, the mass center and the inertia matrix. Usually at the mounting-design stage, the power-train has already been designated, which means the inertia parameters and the excitations are given, then different mounting systems will produce different dynamic force responses in the mounts. The smaller the forces are, the smaller their influence is on the vehicle. So theoretically the dynamic force response levels can be used as evaluation indices of the vibration isolation performance of PMSs.

There are several relevant coordinate systems in the vibration analysis of a PMS shown in Fig. 2. The first is the engine crankshaft coordinate system $O_e x_e y_e z_e$ for power-trains with combustion engines: the origin is the intersection point of the crankshaft center line through the face of the engine rear end. The axis x_e is parallel with the crankshaft center line, and the positive direction is toward the engine front. The axis z_e is parallel with the cylinder center line, pointing to the cylinder head. The axis y_e is determined by the right-hand rule, which should be perpendicular to the center plane of the cylinders, pointing to the engine right. For electric vehicles, this coordinate system can be defined similarly with the driven shaft axis as x_e. The second is the power-train centroid coordinate system $O_c x_c y_c z_c$: the origin is at the power-train mass center. The axes x_c, y_c, z_c are parallel with x_e, y_e, z_e respectively, with the same directions. The third is the local fixed coordinate system $O_i x_i y_i z_i$ of the mount i (i=1-n, n is the number of the mounts): the origin O_i is at the elastic center of the ith mount, and the axes x_i, y_i, z_i are parallel with x_e, y_e, z_e respectively. The last is the principal elastic coordinate system $O_i u_i v_i w_i$ of the mount i: the origin is the same with $O_i x_i y_i z_i$, and the axes u_i, v_i, w_i are parallel with the principal elastic axes of the ith mount respectively. Here suppose the foundation is rigid, all the stiffness of the mounts are invariant with displacements, and the small movements of the elastic centers and principal axes of the mounts during vibrations are neglected as well as the damping effects.

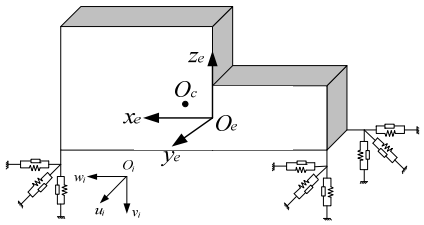

Figure 2. A PMS model and its coordinate systems

The pulsating torques and inertial forces are the main excitations causing the rigid body vibrations of a power-train. Assuming M_u (u=1, 2, ⋯, U) and F_v (v=1, 2, ⋯, V) are the uth pulsating torque and the vth inertial force exerted on the powertrain respectively, and the vibration responses in mount i are the dynamic forces R_{ix}, R_{iy}, R_{iz} in direction x_i, y_i, z_i, respectively. R_{ix}, R_{iy}, R_{iz} can be taken as direct evaluation indices of the vibration isolation performance of a PMS. However, the exact values of the force responses in the mounts are difficult to get by calculation. In the design process, normally the power-train has already been designated and the excitations are given, so we can use a relative quantity Generalized Force Transmissibility (GFT) as the evaluation index. For a system with 1 degree of freedom, 1 input channel and 1 output channel, the force transmissibility is the amplitude ratio of the output force transmitted through the isolator to the input force exerted on the system [11]. For a Multi-Input-Multi-Output (MIMO) system with multi degrees of freedom such as a PMS, we can define the GFT functions referring to the force transmissibility definition as follows:

$$\begin{cases} T_{M_u}^{R_{ix}} = R_{ix}/M_u & T_{M_u}^{R_{iy}} = R_{iy}/M_u & T_{M_u}^{R_{iz}} = R_{iz}/M_u \\ T_{F_v}^{R_{ix}} = R_{ix}/F_v & T_{F_v}^{R_{iy}} = R_{iy}/F_v & T_{F_v}^{R_{iz}} = R_{iz}/F_v \end{cases}$$

These GFT functions have the following characteristics:

(1) They provide a clear demonstration of the vibration isolation performance of a PMS, without involving the calculation of excitations or tests.

(2) They reflect the dynamic force transmitting characteristics of a MIMO vibrational system with rigid bodies and multi degrees of freedom. Under the same excitations, the smaller the GFT is, the smaller the force response is of the corresponding mount and direction.

(3) If the system inputs are dynamic forces, the GFT functions are non-dimensional. If the system inputs are dynamic torques, the GFT functions have dimensions of m^{-1}.

(4) For a time-invariant linear system, the GFT functions are irrelevant with the amplitudes and phases of the excitations, but only depend on the inertia parameters, the stiffness and the damping of the system.

(5) If the type of excitation, such as the amplitude, the direction or the location changes, the GFT can be modified referring to the method above.

Taking an inline 4-cylinder engine for example, the main excitations are the torques of the 2nd order M_{x2} and the 4th order M_{x4} (the directions of which are both around the crankshaft center line), and the force of the 2nd order F_{z2} (along the cylinder center line). Assuming the system inputs are M_{x2}, M_{x4} and F_{z2} respectively, the GFT functions are defined as follows:

$$\begin{cases} T_{M_{x2}}^{R_{ix}} = R_{ix}/M_{x2} & T_{M_{x2}}^{R_{iy}} = R_{iy}/M_{x2} & T_{M_{x2}}^{R_{iz}} = R_{iz}/M_{x2} \\ T_{M_{x4}}^{R_{ix}} = R_{ix}/M_{x4} & T_{M_{x4}}^{R_{iy}} = R_{iy}/M_{x4} & T_{M_{x4}}^{R_{iz}} = R_{iz}/M_{x4} \\ T_{F_{z2}}^{R_{ix}} = R_{ix}/F_{z2} & T_{F_{z2}}^{R_{ix}} = R_{iy}/F_{z2} & T_{F_{z2}}^{R_{ix}} = R_{iz}/F_{z2} \end{cases} \quad (1)$$

B. Optimal Design Objective: Sum of Generalized Force Transmissibility Integrals

The GFT functions are variable in the frequecy domain, but their integrals can reflect the overall transmissbility on their frequency ranges. Assuming the frequency range of M_u is $(f_1^{M_u}, f_2^{M_u})$, and the frequency range of F_v is $(f_1^{F_v}, f_2^{F_v})$, the Generalized Force Transmissibility Integrals (GFTIs) of M_u to R_{ix}, R_{iy}, R_{iz} of the ith mount on $(f_1^{M_u}, f_2^{M_u})$ are

$$A_{ix} = \int_{f_1^{M_u}}^{f_2^{M_u}} T_{M_u}^{R_{ix}}, \; A_{iy} = \int_{f_1^{M_u}}^{f_2^{M_u}} T_{M_u}^{R_{iy}}, \; A_{iz} = \int_{f_1^{M_u}}^{f_2^{M_u}} T_{M_u}^{R_{iz}}$$

and the GFTIs of F_v to R_{ix}, R_{iy}, R_{iz} of the ith mount on $(f_1^{F_v}, f_2^{F_v})$ are

$$B_{ix} = \int_{f_1^{F_v}}^{f_2^{F_v}} T_{F_v}^{R_{ix}}, B_{iy} = \int_{f_1^{F_v}}^{f_2^{F_v}} T_{F_v}^{R_i y}, \; B_{iz} = \int_{f_1^{F_v}}^{f_2^{F_v}} T_{F_v}^{R_{iz}}$$

The Sum of Generalized Force Transmissibility Integrals (SGFTI) can be defined as

$$J_{M_u} = \sum_{i=1}^{n} \left(a_{ix} \cdot A_{ix} + a_{iy} \cdot A_{iy} + a_{iz} \cdot A_{iz} \right) \quad (2)$$

$$J_{F_v} = \sum_{i=1}^{n} \left(b_{ix} \cdot B_{ix} + b_{iy} \cdot B_{iy} + b_{iz} \cdot B_{iz} \right) \quad (3)$$

In the expressions, a_{ix}, a_{iy}, a_{iz}, b_{ix}, b_{iy}, b_{iz} are weighing coefficients, the values of which can be set according to the importance of each transmissibility. Commonly they can take the value of 0 or 1.

The integration of the GFT function on a specified range of frequency equals the area between the function curve and the frequency axis, so the GFTI should be a scalar. Dividing it by the length of the frequency range, a new quantity will be get presenting the average GFT level on this frequency range. The smaller the GFTI is, the smaller the average GFT level is, and the better the vibration isolation performance is in the corresponding direction of the corresponding mount. The optimization objective is to seek the minimization of each J_{Mu} and J_{Fv} of equal importance. But a multi-objective optimization is usually more difficult than a single-objective optimization when the solution method and calculation workload are concerned, so commonly we can transform it into an equivalent single-objective problem to solve. The new objective function can be defined as

$$J = \sum_{u=1}^{U} \lambda_u J_{M_u} + \sum_{v=1}^{V} \lambda_v' J_{F_v} \quad (4)$$

In this function λ_u and λ_v' are coefficients weighing J_{Mu} and J_{Fv} into functions with the same order of magnitude. If they already have the same order, λ_u and λ_v' can take the value of 1. J is also a scalar. Therefore, the multi-objective optimization problem involving multiple GFT functions of different excitation types, different mounts and different orthogonal directions is transformed into a single-objective optimization problem. In this way, the mounts and directions of higher GFT values and the excitation types of broader frequency ranges in the original system will actually be paid special attention to, making the SGFTI have an automatic weighing ability. The optimization will minimize the overall GFT level of the mounting system over the specified frequency ranges. If there are special requirements on the GFT of a specific mount in a specific direction under a specific type of excitation, the weighing coefficients in (2)-(3) can be set with desired values.

Without loss of generality, take the most commonly used inline 4-cylinder engine for example. During the engine operating speed, if the frequency range of the 2nd order torque and force is $(f_1^{M_{x2}}, f_2^{M_{x2}})$, and the frequency range of the 4th order torque is $(f_1^{M_{x4}}, f_2^{M_{x4}})$, there should be relationships that $f_1^{M_{x4}} = 2 f_1^{M_{x2}}$, $f_2^{M_{x4}} = 2 f_2^{M_{x2}}$, and normally $f_2^{M_{x2}} > f_1^{M_{x4}}$. At the same time and the same speed, the amplitude, the frequency and the phase of M_{x2} are different with those of M_{x4} respectively, but their directions are both around the crankshaft centerline. For a linear system, the GFT function is irrelevant with the amplitudes

and phases of excitations, so here we use M_x as a uniform expression for M_{x2} and M_{x4}, and unite their frequency ranges to $(f_1^{M_{x2}}, f_2^{M_{x4}})$, covering the frequency of the 2nd and the 4th order torques during the engine speed. Meanwhile use F_z as a substitution of F_{z2} for the uniformity of expression.

Supposing $A_{ix} = \int_{f_1^{M_{x2}}}^{f_2^{M_{x4}}} T_{M_x}^{R_{ix}}$, $A_{iy} = \int_{f_1^{M_{x2}}}^{f_2^{M_{x4}}} T_{M_x}^{R_i y}$, $A_{iz} = \int_{f_1^{M_{x2}}}^{f_2^{M_{x4}}} T_{M_x}^{R_{iz}}$ are the Generalized Force Transmissibility Integrals (GFTIs) of M_x to R_{ix}, R_{iy}, R_{iz} of the ith mount on $(f_1^{M_{x2}}, f_2^{M_{x4}})$, and $B_{ix} = \int_{f_1^{M_{x2}}}^{f_2^{M_{x2}}} T_{F_z}^{R_{ix}}$, $B_{iy} = \int_{f_1^{M_{x2}}}^{f_2^{M_{x2}}} T_{F_z}^{R_{iy}}$, $B_{iz} = \int_{f_1^{M_{x2}}}^{f_2^{M_{x2}}} T_{F_z}^{R_{iz}}$ are the GFTIs of F_z to R_{ix}, R_{iy}, R_{iz} of the ith mount on $(f_1^{M_{x2}}, f_2^{M_{x2}})$, according to (2)-(3), the SGFTI are

$$J_{M_x} = \sum_{i=1}^{n} \left(a_{ix} \square A_{ix} + a_{iy} \square A_{iy} + a_{iz} \square A_{iz} \right) \tag{5}$$

$$J_{F_z} = \sum_{i=1}^{n} \left(b_{ix} \square B_{ix} + b_{iy} \square B_{iy} + b_{iz} \square B_{iz} \right) \tag{6}$$

According to (4), the objective function can be defined as

$$J = J_{M_x} + \lambda J_{F_z} \tag{7}$$

For other kinds of power units, the GFTIs and SGFTI can be defined according to the amount and types of excitations. The frequency ranges should also be set according to the circumstances.

C. Optimal Design Algorithm

Clearly the relations between the objective of SGFTI and the mounting parameters are nonlinear. The Generalized Reduced Gradient (GRG) algorithm can be used in the calculation of this nonlinear single-objective optimal design process. The GRG algorithm is one of the most effective algorithms in solving nonlinear programming problems at present. This algorithm distinguishes the variables into basic variables and non-basic variables, and expresses the former ones with the latter ones using constraint conditions. So it can reduce the feasible space dimension of the objective function, and simplify the nonlinear constraint problem into an ordinary constraint problem. Consider the nonlinear programming problem

$$\min f(\boldsymbol{x}) \quad (\boldsymbol{x} \in \boldsymbol{R}^n)$$

$$\text{s.t.} \quad \boldsymbol{h}(\boldsymbol{x}) = 0 \quad (\boldsymbol{h} \in \boldsymbol{R}^m, \ m \le n)$$

$$\boldsymbol{l} \le \boldsymbol{x} \le \boldsymbol{u} \quad (\boldsymbol{l}, \boldsymbol{u} \in \boldsymbol{R}^n)$$

In the equations, there is $\boldsymbol{h}(\boldsymbol{x}) = (h_1(x), \cdots, h_m(x))^T$. Given $\boldsymbol{x} = (\boldsymbol{x}_B^T, \boldsymbol{x}_N^T)^T$, $\boldsymbol{l} = (\boldsymbol{l}_B^T, \boldsymbol{l}_N^T)^T$, and $\boldsymbol{u} = (\boldsymbol{u}_B^T, \boldsymbol{u}_N^T)^T$, $\boldsymbol{x}_B \in \boldsymbol{R}^m$ are basic variables, $\boldsymbol{x}_B$ are non-basic variables. If the Jacobi matrix of $\boldsymbol{h}(\boldsymbol{x})$ is

$$\frac{\partial \boldsymbol{h}}{\partial \boldsymbol{x}} = \left(\frac{\partial \boldsymbol{h}}{\partial \boldsymbol{x}_B}, \frac{\partial \boldsymbol{h}}{\partial \boldsymbol{x}_N} \right)$$

Then the GRG is

$$\boldsymbol{r}(\boldsymbol{x}_N) = \nabla_{\boldsymbol{x}_N} f - \left[\left(\frac{\partial \boldsymbol{h}}{\partial \boldsymbol{x}_B} \right)^{-1} \frac{\partial \boldsymbol{h}}{\partial \boldsymbol{x}_N} \right]^T - \nabla_{\boldsymbol{x}_B} f$$

In the equations, there are $\nabla_{x_B} f = (\frac{\partial f}{\partial x_1}, \ldots, \frac{\partial f}{\partial x_m})^T$ and $\nabla_{x_N} f = (\frac{\partial f}{\partial x_1}, \ldots, \frac{\partial f}{\partial x_n})^T$.

Taking the negative direction of the GRG as the searching direction, the objective value will be reduced by an iterative process until the minimum is achieved. The gradient of the objective function can be calculated using forward difference or central difference in numerical calculation. Detailed introduction of this algorithm can be found in reference [12].

D. Characteristics of the GFT Method

The GFT method considers a PMS as a MIMO system. The definition of SGFTI takes all the excitations, all the forces transmitted through all the mounts in all the 3 directions of a PMS into account in a weighed form, which can be adjusted according to the real case. Besides, by selecting the upper limits and lower limits of the integrations properly, the system GFT level can be lowered in desired frequency ranges, and thus improve the vibration isolation performance of the PMS in a comprehensive way.

III. DISCUSSIONS OF THE GFT METHOD

Take a typical 3-point PMS of a rear-engined vehicle for example as shown in Fig. 3. The GFT functions and the SGFTI will be defined, and then the optimization will be performed to investigate the characteristics of the method. The power-train has a longitudinally fitted inline 4-cylinder combustion engine and a 3-point mounting system. In the original design, both the 2 front mounts are symmetrically positioned under the engine side with 45 degree angles, and the rear mount is above the transmission box, all of which are ordinary rubber mounts. The power-train is mounted on a thick and firm frame, so here we temporarily suppose the foundation is rigid. The effect of a more compliant foundation will be considered in the next research [13]. The dynamic model of the system is built with multi-body dynamics analysis software ADAMS.

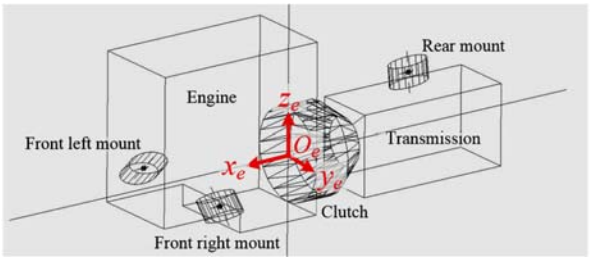

Figure 3. The dynamic model of a PMS

A. *Definitions about the Design Objective*

In the engine crankshaft coordinate system, the GFT functions of the *i*th mount (*i*=1, 2, 3) are defined as

$$\begin{cases} T_{M_x}^{R_{ix}} = R_{ix} / M_x \quad T_{M_x}^{R_{iy}} = R_{iy} / M_x \quad T_{M_x}^{R_{iz}} = R_{iz} / M_x \\ T_{F_z}^{R_{ix}} = R_{ix} / F_z \quad T_{F_z}^{R_{iy}} = R_{iy} / F_z \quad T_{F_z}^{R_{iy}} = R_{iz} / F_z \end{cases}$$

The engine idle speed is 800r/min, and the range of its working speed is 800-2800 r/min, so the frequency range of M_x is 25-190 Hz (combing the frequency range of the 2nd order and the 4th order torques), and that of F_z is 25-95 Hz. But the frequencies of the excitations in the higher range (50-190Hz) have been far away from the modal frequencies of power-train rigid-body vibrations, and caculation results show that the values of all the GFT functions above 50Hz are much smaller than those between 25-50Hz, which means the area representing the GFTIs above 50Hz only occupy a very small part of the overall area, so in this case we uniformly use 25-50Hz as the frequency range in the optimization.

Supposing $A_{ix} = \int_{25}^{50} T_{M_x}^{R_{ix}} df$, $A_{iy} = \int_{25}^{50} T_{M_x}^{R_{iy}} df$, $A_{iz} = \int_{25}^{50} T_{M_x}^{R_{iz}} df$ are the GFTIs of M_x to R_{ix}, R_{iy}, R_{iz} of the *i*th mount on the frequency range 25-50 Hz respectively, and $B_{ix} = \int_{25}^{50} T_{F_z}^{R_{ix}} df$, $B_{iy} = \int_{25}^{50} T_{F_z}^{R_{iy}} df$, $B_{iz} = \int_{25}^{50} T_{F_z}^{R_{iz}} df$ are the GFTIs of F_z to R_{ix}, R_{iy}, R_{iz} of the *i*th mount on the frequency range 25-50 Hz respectively, the SGFTI and the design objective J can be defined as in (5)-(7). In a trial calculation, J_{M_x} and J_{F_z} have the same dimension, so λ will take the value of 1.

B. *Selections of the Design Variables*

In a mounting system, the variables affecting the rigid-body natural vibration characteristics include: the dynamic stiffness k_{ui}, k_{vi}, k_{wi} along 3 principal elastic axes u_i, v_i, w_i of each mount, the elastic center coordinates x_i, y_i, z_i of each mount in the engine crankshaft coordinate system, and the inclination angles of each principal elastic axis of each mount in the engine crankshaft coordinate system. All these design parameters could be used as the optimization variables. Generally, the damping effects of an ordinary rubber mount are relatively small, and difficult to be considered as design variables in the optimization, but appropriate values should be given to avoid the peaks in the GFT function curves. As for the inclination angles, this example takes the angles θ_1 and θ_2 between the axes w_i and z_i of both the front mounts and θ_3 between the axes u_i and z_i of the rear mount as the design variables, because these angles can be easily realized by the design of frames and brackets of the mounts after the optimization. The 21 design variables chosen are shown in Table I.

TABLE I. THE DESIGN VARIABLES CHOSEN

Number	Design variable	Lower limit	Upper limit
1	The elastic center coordinate of the front left mount x_1 (mm)	–250	250
2	The elastic center coordinate of the front left mount y_1 (mm)	–100	100
3	The elastic center coordinate of the front left mount z_1 (mm)	–100	100
4	The elastic center coordinate of the front right mount x_2 (mm)	–250	250
5	The elastic center coordinate of the front right mount y_2 (mm)	–100	100
6	The elastic center coordinate of the front right mount z_2 (mm)	–100	100
7	The elastic center coordinate of the rear mount x_3 (mm)	–250	250
8	The elastic center coordinate of the rear mount y_3 (mm)	–100	100
9	The elastic center coordinate of the rear mount z_3 (mm)	–100	100
10	The inclination angle of the front left mount θ_1 (°)	–35	5
11	The inclination angle of the front right mount θ_2 (°)	–35	5
12	The inclination angle of the rear mount θ_3 (°)	–5	85
13	The stiffness of the front left mount in *u* direction k_{u1} (%)	–50%	100%
14	The stiffness of the front left mount in *v* direction k_{v1} (%)	–50%	100%
15	The stiffness of the front left mount in *w* direction k_{w1} (%)	–50%	100%
16	The stiffness of the front right mount in *u* direction k_{u2} (%)	–50%	100%
17	The stiffness of the front right mount in *v* direction k_{v2} (%)	–50%	100%
18	The stiffness of the front right mount in *w* direction k_{w2} (%)	–50%	100%
19	The stiffness of the rear mount in *u* direction k_{u3} (%)	–50%	100%
20	The stiffness of the rear mount in *v* direction k_{v3} (%)	–50%	100%
21	The stiffness of the rear mount in *w* direction k_{w3} (%)	–50%	100%

C. *Constraint Conditions*

(1) The frequency constraints

A reasonable distribution of the modal frequencies is one of the most important aspects in the design of a PMS. Generally speaking, the modal frequency of the highest order should be much lower than the excitation frequency of the primary order at the engine idle speed, and the ratio of the latter to the former (usually called the frequency ratio)

should commonly be greater than $\sqrt{2}$, in case that the pulsating torques and inertial forces excited the resonance of the power-train. But if the mounts are too flexible, large movements of the power-train could be excited by impacts and excitations in lower frequencies, and the life of the mounts could be affected. So the modal frequency of the lowest order should also be limited. Considering the factors above, set the frequency constraint of the highest order as $f_6 \leq 16.5$ Hz, and the lowest order as $f_1 \geq 4.5$ Hz.

(2) The constraints of the design variables

The constraints of the design variables should also be set in order to keep them within a feasible design space to satisfy the design requirements in the following design process of the mounts. Acording to the acual condition in the vehicle, the allowed ranges of the design variables in this optimization are shown in Table I. In this table, the values of the upper limits and the lower limits of the elastic center coordinates and the inclination angles are the allowed amounts of changes relative to the original design. Those of the stiffness are the allowed percentages of changes relative to the original design.

This optimization method pursues the reduction of the GFT level of the mounting system, so other commonly used constraints such as the MKE are no longer applied.

D. Analysis of the Optimization Results with Full Constraints

To make the results meet the practical circumstances on the vehicle, an optimization with full constraints is carried out from the original design considering all those conditions listed in *C*.

(1) The design objective. As in Fig. 4, after 19 iterations, the SGFTI *J* drops to 7.8 from 26.0 before the optimization. The changes of the GFT functions in 3 directions of each mount before and after the optimization are shown in Fig. 5(a) - (f). In order to show the changes more clearly before and after the optimization, the unit of the GFT on the longitudinal axis adopts dB.

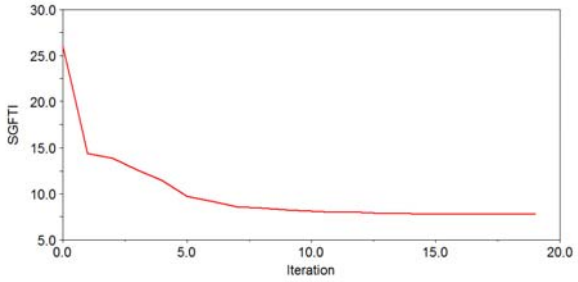

Figure 4. Changes of the SGFTI in the optimization

The original design is the mounting system before the optimization on the vehicle. According to the figures, the GFT functions of most mounts in most directions have decreased after the optimization. The mounts having higher GFT levels in the original design generally get greater reduction. Some special mounts in some individual directions have a little increase, mostly when the GFT values are relatively small, including the GFTs of M_x in direction z of the front left mount and the rear mount, and the GFT of F_z in direction z of the rear mount.

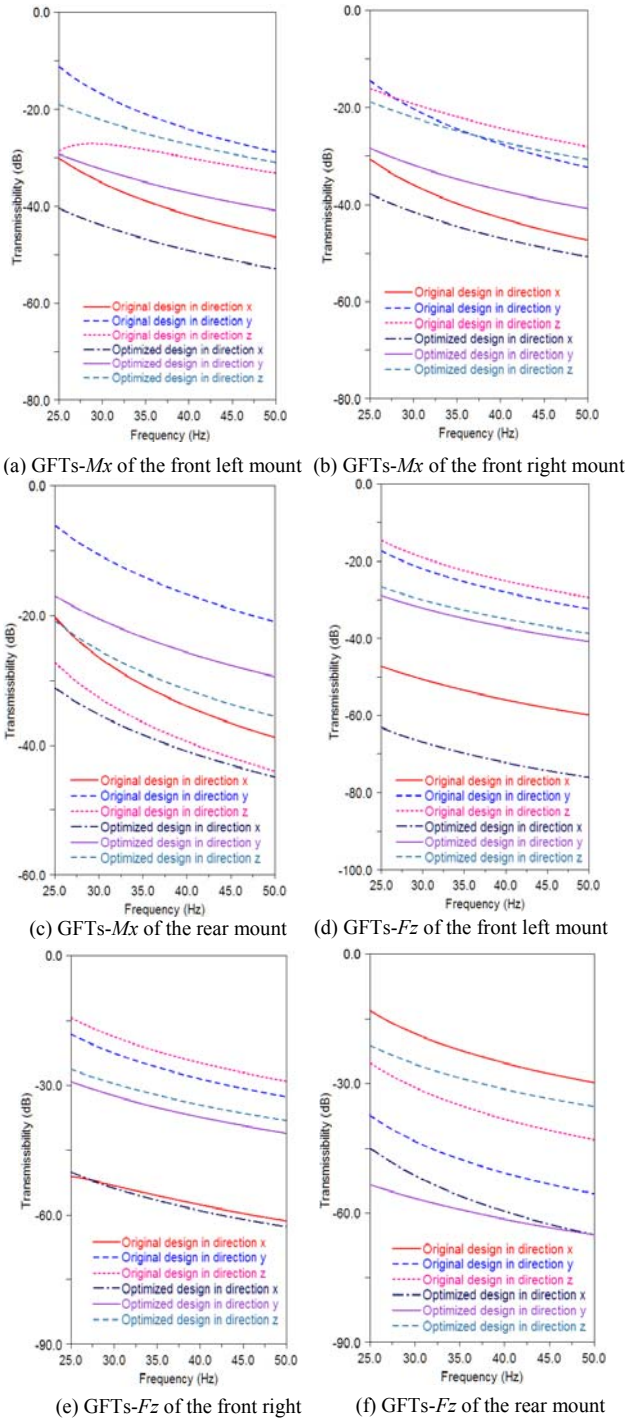

(a) GFTs-*Mx* of the front left mount (b) GFTs-*Mx* of the front right mount

(c) GFTs-*Mx* of the rear mount (d) GFTs-*Fz* of the front left mount

(e) GFTs-*Fz* of the front right (f) GFTs-*Fz* of the rear mount

Figure 5. The GFTs of each mount before and after the optimization

(2) The modal frequencies and MKE distribution. The modal frequencies of the PMS before and after the optimization are shown in Table II. The frequency ratio δ

is the ratio of the excitation frequency of the 2nd primary order in idling speed to each of the modal frequencies of the system.

TABLE II. THE MODAL FREQUENCIES OF THE PMS BEFORE AND AFTER THE OPTIMIZATION

Order	Before optimization		After optimization	
	Modal frequency f (Hz)	Frequency ratio δ	Modal frequency f (Hz)	Frequency ratio δ
1	4.80	5.6	4.50	5.9
2	9.30	2.9	5.16	5.2
3	10.81	2.8	6.93	3.9
4	11.20	2.4	7.87	3.4
5	15.73	1.7	9.11	2.9
6	16.41	1.6	14.22	1.9

After optimization, all the modal frequencies have got obvious reductions. The frequency of the highest order has a reduction more than 2Hz, and its value is closed to 1/2 of the 2nd primary order frequency in idling speed. The frequency of the lowest order reaches the lower limit of the frequency constraint (4.5Hz). The frequency reduction is an important factor making the GFT functions decrease in lower frequencies.

The MKE distribution before and after the optimization are shown in Table III (a)-(b).

TABLE III. THE MKE DISTRIBUTION OF THE PMS

(a) BEFORE OPTIMIZATION

Order		1	2	3	4	5	6
Frequency (Hz)		4.8	9.3	10.81	11.2	15.73	16.41
Modal Kinetic Energy Distribution (%)	x	0.00	2.10	5.39	73.22	14.72	4.51
	y	44.74	0.01	45.55	4.06	1.93	3.15
	z	0.01	86.58	1.21	6.32	4.38	1.48
	α	37.88	0.01	44.98	4.53	1.79	10.26
	β	0.02	11.29	2.26	11.80	54.53	20.07
	γ	17.35	0.00	0.60	0.07	22.65	60.54

(b) AFTER OPTIMIZATION

Order		1	2	3	4	5	6
Modal Kinetic Energy Distribution (%)	x	0.00	1.60	9.41	68.33	5.57	11.59
	y	57.06	0.40	39.03	5.77	3.05	2.39
	z	0.19	81.82	0.46	7.94	2.43	5.72
	α	36.23	0.01	46.26	7.55	15.24	7.93
	β	0.01	16.15	3.82	10.18	17.81	41.24
	γ	6.51	0.03	1.01	0.24	55.91	31.13

Comparing the MKE distributions before and after the optimization, it can be seen that there is no clear and regular patterns that the MKE distribution changes. No mode is fully decoupled from other modes due to the limited design space on the vehicle.

(3) The design variables. The values of the design variables before and after the optimization with full constraints are shown in Table IV. The names of the variables can be referred in Table I.

It can be seen that almost every variable has changed after the optimization. All the stiffness values have reached their lower limits given in Table I. It indicates that the reduction of mount stiffness (and simultaneously the reduction of modal frequencies) is the main factor that the SGFTI is lowered after the optimization. Fig. 6 is the final mounting scheme.

TABLE IV. THE VALUES OF THE DESIGN VARIABLES BEFORE AND AFTER THE OPTIMIZATION

Number	Unit	Before optimization	Optimization with full constraints	Optimization with less constraints
1	mm	566	341	413
2	mm	-261	-264	-94
3	mm	-54	46	166
4	mm	566	316	332
5	mm	261	361	-86
6	mm	-54	-119	153
7	mm	-682	-735	-437
8	mm	0	33	9
9	mm	297	197	7
10	°	45	50	40
11	°	45	50	45
12	°	5	75	42
13	N/mm	191	95.3	165
14	N/mm	261	130.5	173
15	N/mm	1382	690.8	767
16	N/mm	191	95.3	181
17	N/mm	261	130.5	133
18	N/mm	1382	690.8	1033
19	N/mm	3627	1813.5	2546
20	N/mm	572	286.0	328
21	N/mm	998	499.9	630

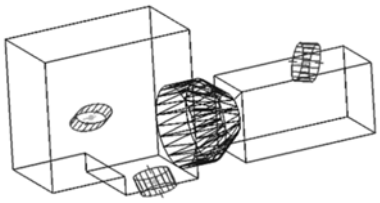

Figure 6. The mounting scheme after the optimization with full constraints

E. Analysis of the Optimization Results With Fewer Constraints

In order to fully investigate the properties of this optimal design method, an optimization with fewer constraints is then performed. The frequency constraints, the allowed ranges of the elastic center coordinates and the inclination angles are temporarily removed. But the ranges of the mount stiffness are still kept to avoid the stiffness approaching 0 in the optimization.

(1) The design objective. After 20 iterations, the SGFTI J drops significantly to 0.3 from 26.0 before the optimization.

The changes of the GFT functions in 3 directions of each mount before and after the optimization are shown in Fig. 7(a)-(f).

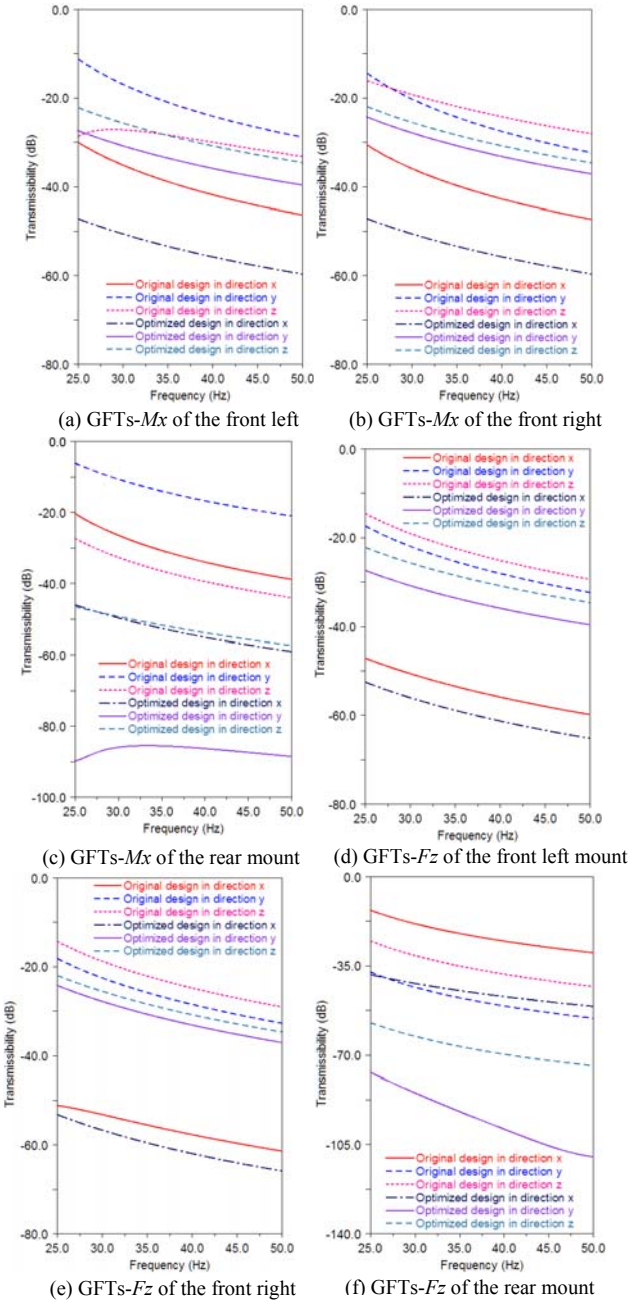

(a) GFTs-*Mx* of the front left (b) GFTs-*Mx* of the front right

(c) GFTs-*Mx* of the rear mount (d) GFTs-*Fz* of the front left mount

(e) GFTs-*Fz* of the front right (f) GFTs-*Fz* of the rear mount

Figure 7. The GFTs of each mount before and after the optimization

According to Fig. 7, almost all the GFT functions have dropped obviously after the optimization, especially in those directions where the GFT levels are higher in the original design, such as the GFTs of M_x in direction y of all the 3 mounts, the GFTs of F_z in direction z of all the 3 mounts, and the GFT of F_z in direction x of the rear mount. This also illustrates the automatic weighing ability of this method. Only the GFT of M_x in direction z of the front left mount have a slight increase in the lower frequency range of 25-40Hz.

(2) The modal frequencies and the MKE distribution after the optimization are shown in Table II.

Compairing Table V with Table III (a) it can be seen that all the modal frequencies of the system have decreased significantly compared to the original design, especially the 1st order, which drops from 4.8Hz to 0.03Hz. Furthermore, the mode of the 1st order is almost fully decoupled in direction α, with its MKE percentage reaching 91.31%, compared to the original one never exceeding 50% in each mode before optimization. However, there are no obviously decoupled modes in other directions after the optimization. The modal frequencies are moved further away from the frequency ranges of excitations, and the decoupling of the TRA mode can also improve the vibration isolation performance referring to the study before [5], both of which together lower the system GFT level greatly. It can be seen that given enough design space, a typical PMS just reaches a TRA decoupled system after the optimization with the GFT method.

TABLE V. THE FREQUENCIES AND THE MKE DISTRIBUTION AFTER THE OPTIMIZATION

order		1	2	3	4	5	6
Frequency (Hz)		0.03	4.64	6.06	8.51	9.55	11.93
Modal Kinetic Energy Distribut -ion (%)	x	0.09	0.33	61.96	0.05	0.60	36.94
	y	0.00	48.89	0.30	39.93	10.67	0.05
	z	2.70	0.31	15.74	9.29	36.09	35.85
	α	91.31	0.16	0.41	4.58	3.82	0.02
	β	5.86	0.03	21.20	7.77	38.01	27.12
	γ	0.04	50.28	0.39	38.38	10.81	0.02

(3) The design variables. The values of the design variables before and after the optimization are shown in Table IV.

It is shown that almost all the variables have changed obviously after the optimization. All the stiffness values of the mounts have decreased significantly, but none of them reaches its lower limit except the stiffness of the front right mount in v direction. In Fig. 8, it is shown that the elastic centers of the front left mount and the front right mount are close (82mm) to each other after the optimization. If we pick the midpoint between the elastic centers of the 2 front mounts, the line between this point and the elastic center of the rear mount is very close to the mass center of the power-train (32.5mm), and its angles are very close to those of the TRA of the power-train, as shown in Table VI. Obviously, with the cooperation of the optimized mount stiffness (lowered but not to the lower limit), this type of scheme can

achieve smaller torsional stiffness about the TRA, and thus decouple the TRA mode and reduce modal frequencies. Since the angle between the TRA and the axis x_e is relatively small (10.77°), the modal energy percentage in direction α is also raised.

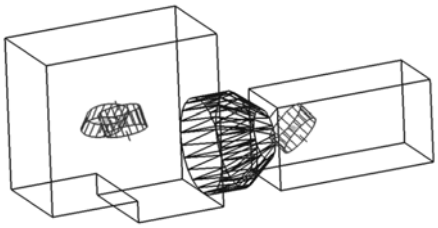

Figure 8. The mounting scheme after the optimization with fewer constraints

TABLE VI. THE ANGLES BETWEEN THE LINE AND THE COORDINATE AXES

Line	θ_1 (°)	θ_2 (°)	θ_3 (°)
The Torque Roll Axis of the power-train	10.77	91.62	79.36
The line between the front mounts and the rear mount	12.66	96.85	79.41

θ_1、θ_2 and θ_3 are the angles between the lines and the coordinate axes x_e、y_e and z_e respectively.

F. Running Tests on Vehicle

After the optimization with full constraints, mounts and their brackets are redesigned and installed on the bus according to the optimal results.

As shown in Table IV, the stiffness values of all the mounts in 3 directions are nearly half of the original ones after the optimization, so rubber material with lower Shore hardness is used in the new mounts, and the shapes and frames are also adjusted as shown in Fig. 9(a)-(b). Deformations after installation are still in the permissible ranges.

(a) The original design (left) and the new design (right) of the front mount

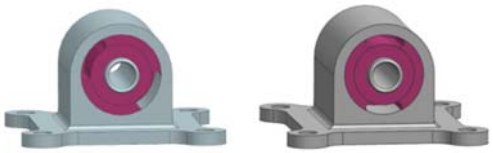

(b) The original design (left) and the new design (right) of the rear mount

Figure 9. The original design and the new design of the mounts

The positions and the orientations of the mounts are realized by the redesign of the frames and brackets as shown in Fig.10.

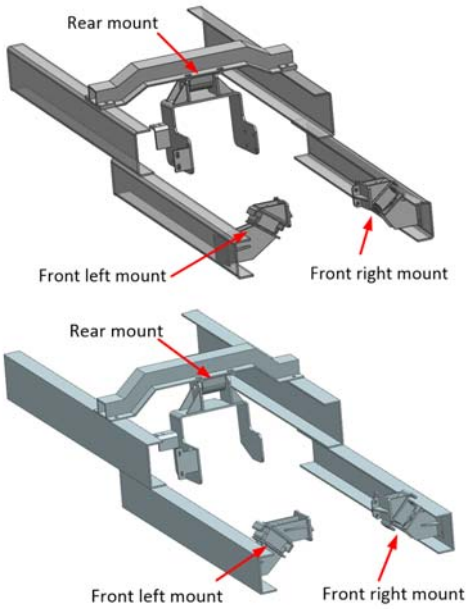

Figure 10.The original design (left) and the new design (right) of the brackets

Idling and on-road tests are done to compare the vibration isolation performance of the new mounting system and the original one on the bus as shown in Fig. 11. The data collection system is Iotech WaveBook 512 with 8 channels, and the accelerometers are B&W BW14105, as shown in Fig. 12. Two sensors are set on the cushions of the seats on the 3rd row and the last row respectively to measure the accelerations on 3 axis, and another 2 sensors are set on the floor and the body near the seat of the last row to measure the acceleration on z axis. The Root Mean Squares (RMSs) of accelerations are collected at each measure point when the vehicle is idling and running on smooth road at certain speeds, as shown in Table VII. Signals of 10 seconds at least are recorded in each state.

Figure 11.The bus on which the mounting system is installed

Figure 12.The data collection system and the accelerometer

TABLE VII. RMSs OF ACCELERATIONS AT THE MEASURE POINTS BEFORE AND AFTER THE OPTIMIZATION

Measure point	Before optimization			After optimization		
	100 km/h	60 km/h	idling	100 km/h	60 km/h	idling
Seat on the 3rd row- *x* (m/s^2)	0.954	0.802	0.216	0.701	0.525	0.138
Seat on the 3rd row - *y* (m/s^2)	0.857	0.921	0.226	0.513	0.749	0.171
Seat on the 3rd row- *z* (m/s^2)	1.147	0.975	0.126	0.984	0.634	0.132
Seat on the last row- *x* (m/s^2)	0.494	0.618	0.365	0.453	0.447	0.263
Seat on the last row - *y* (m/s^2)	1.459	0.803	0.197	0.936	0.538	0.122
Seat on the last row - *z* (m/s^2)	0.908	0.715	0.070	0.851	0.673	0.114
Floor under the seat on the last row - *z* (m/s^2)	1.442	1.386	0.734	1.040	0.975	0.829
Body near the seat on the last row - *z* (m/s^2)	0.264	0.287	0.207	0.171	0.165	0.192

It can be seen that the RMSs of accelerations at most points in most directions have decreased significantly, except for the seat on the 3rd row, the seat on the last row and the floor under this seat in *z* direction when idling, but these values aren't notable compared with other directions, and their increments are even smaller.

G. Discussions

Through the opimizations, the GFT method shows different properties and a certain relations with the TRA method and the MKE method:

(1) No matter after the optimization with fewer constraints or with full constraints, the modal frequencies of the system decrease significantly. Lowering the stiffness of the mounting system can bring down the modal frequencies, which is an effective way to reduce the system GFT level.

(2) After the optimization with fewer constraints, the TRA mode is almost fully decoupled. It can be seen that with the concurrent reduction of the modal frequencies, full decoupling of the TRA mode may help with the decrement of the system GFT level.

(3) The changes of MKE distributions after both optimizations have no regular patterns except for the TRA mode after the optimization with fewer constraints, which means the decoupling of other modes may not help as much as the 2 factors mentioned above in lowering the system GFT level.

(4) In confined design space, the TRA mode may not be fully decoupled, so the reduction of the GFT level does not definitely bring about the increase of the MKE distribution of the TRA mode, for the 2 indices represent different aspects of interests. Larger MKE distribution of the TRA mode does not definitely mean better vibration isolation performance when it cannot be fully decoupled.

IV. CONCLUSIONS

(1) The GFT functions reflect the vibration characteristics of MIMO systems. Their meanings are clearer, and their values are easier to get without difficult calculations, so they are appropriate to be used as indices of vibration isolation performance of a PMS. The SGFTI transforms the GFT functions of all the mounts in all 3 directions into a scalar value, which can be used as an optimal design objective. By adding the GFT integral of each mount in each direction in a weighed form together, a complex multi-objective optimization problem can be transformed into a simple single-objective optimization problem with automatic weighing ability. The effects of the optimization can be evaluated by the objective value or by the GFT functions of each mount directly. By the weighing method, the GFT of a special mount in a special direction of special attention can be optimized specially.

(2) The GFT method not only considers all the excitations, all the forces transmitted through the mounts in all the 3 directions, but also takes the frequency ranges into account. The examples show that it can lower the system GFT level in the desired frequency ranges, thus reduce amplitudes of the dynamic forces transmitted to the foundation from frequency domain. So it is a comprehensive optimal design method of PMSs. Using associative functions of ADAMS, the model of a PMS can be established, and the response analysis, the objective definition, the calculation process and the result output can be performed with clear visibility and high efficiency. GRG

algorithm can perform the nonlinear programming calculation, so it is feasible to be used in the GFT method.

(3) The TRA decoupling design method of a mounting system could provide better vibration isolation performance if it can be fully decoupled and the modal frequencies are reduced simultaneously. In the early design stage, when the design variables have enough design space, it is desirable to use this method to determine the scheme of a mounting system. On the other hand, the GFT method can directly lower the GFT level when the TRA mode cannot be fully decoupled in confined design space, and thus imporve the vibration isolation performance, so it is suitable to be used in the improving design stage of a PMS.

ACKNOWLEDGEMENTS

This research is supported by National Natural Science Foundation of China (Grant No. 51405269 and 51375265), Excellent Middle-Aged and Youth Scientist Award Foundation of Shandong Province (Grant No. BS2014ZZ003) and Shandong Provincial Natural Science Foundation, China (Grant No. ZR2016EEM31).

REFERENCES

[1] Kaul S., Dhingra A. Engine mount optimisation for vibration isolation in motorcycles. Vehicle System and Dyanamics, Vol. 47, Issue 4, 2009, p. 419-436.

[2] Tao J.S., Liu G.R., Lam K.Y. Excitation force identification of an engine with velocity data at mounting points. Journal of Sound and Vibration, Issue 242, 2001, p321-331.

[3] El Hafidi A., Martin B., Loredo A., Jego E. Vibration reduction on city buses: Determination of optimal position of engine mounts. Mechanical Systems and Signal Processing, Vol. 24, Issue 7, 2010, p. 2198-2209.

[4] Lu Z.H，Fan R.L, Feng Z.D. A survey of design methods for automotive engine mounting system. Chinese Internal Combustion Engine Engineering, Vol. 25, Issue 3, 2004, p. 37-43.

[5] Jeong T., Singh R. Analytical methods of decoupling the automotive engine torque roll axis. Journal of Sound and Vibration, Issue 234, 2000, p. 85-114.

[6] Xu P., Bernardo B., Tan K. Optimal mounting design for cab vibration isolation. International Journal of Vehicle Design, Vol. 57, Issue 2-3, 2011, p. 292-304.

[7] Zhou M., Hou Z.C. Optimization on engine mounting based on genetic algorithm. Automobile Technology, Issue 9, 2006, p. 13-16.

[8] Yin Q., Gu Z., Tao J., Wu W., Xu Y. Analysis and optimization design of powertrain mounting system of electric drive truck. China Mechanical Engineering, Vol. 24, Issue 20, 2013, p. 2826-2831.

[9] Shangguan W., Wu J. Modelling of dynamic performances for hydraulic engine mounts using fractional derivative and optimisation of powertrain mounting systems. International Journal of Vehicle Design, Vol. 47, Issue 1-4, 2008, p. 215-233.

[10] Madjlesi R., Khajepour A., Ismail F., Wybenga M., Rice B., Mihalic J. Optimisation of engine mounting systems using experimental FRF vehicle model. International Journal of Vehicle Noise and Vibration, Vol. 47, Issue 3-4, 2005, p. 232-250.

[11] William T.T. and Marie D.D. Theory of Vibration with Applications. Fifth Edition, Tsinghua University Press, Beijing, 2005.

[12] Huang H.X. and Han J.Y. Mathematical Programming. Tsinghua University Press. First Edition, Beijing, 2006.

[13] Hu J.F. and Singh R. Improved torque roll axis decoupling axiom for a powertrain mounting system in the presence of a compliant base. Journal of Sound and Vibration, Issue 331, 2012, p. 1498-1518.